



University of Tennessee, Knoxville
**TRACE: Tennessee Research and Creative
Exchange**

Chancellor's Honors Program Projects

Supervised Undergraduate Student Research
and Creative Work

Spring 5-1999

Growth of Silicon Microcolumns by Pulsed Excimer Laser Irradiation *In Vacuo*

Neal Curtis Oldham
University of Tennessee - Knoxville

Follow this and additional works at: https://trace.tennessee.edu/utk_chanhonoproj

Recommended Citation

Oldham, Neal Curtis, "Growth of Silicon Microcolumns by Pulsed Excimer Laser Irradiation *In Vacuo*" (1999). *Chancellor's Honors Program Projects*.
https://trace.tennessee.edu/utk_chanhonoproj/332

This is brought to you for free and open access by the Supervised Undergraduate Student Research and Creative Work at TRACE: Tennessee Research and Creative Exchange. It has been accepted for inclusion in Chancellor's Honors Program Projects by an authorized administrator of TRACE: Tennessee Research and Creative Exchange. For more information, please contact trace@utk.edu.

**Appendix D - UNIVERSITY HONORS PROGRAM
SENIOR PROJECT - APPROVAL**

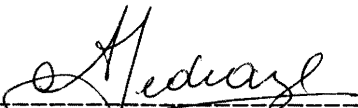
Name: Neal Oldham

College: Engineering Department: Materials Science & Engineering

Faculty Mentor: Anthony Pedraza

PROJECT TITLE: "Growth of silicon microcolumns by
pulsed excimer laser irradiation in-vacuo"

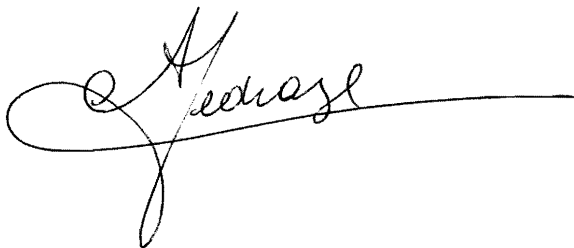
I have reviewed this completed senior honors thesis with this student and certify that it is a project commensurate with honors level undergraduate research in this field.

Signed: , Faculty Mentor

Date: 5/12/99

Comments (Optional):

These is an excellent project and should receive the highest marks.



GROWTH OF SILICON MICROCOLUMNS BY PULSED EXCIMER LASER
IRRADIATION *IN VACUO*

A Thesis
Presented for the
Bachelor of Science
Degree
The University of Tennessee, Knoxville

Neal Oldham
May 1999

ACKNOWLEDGEMENTS

I would like to thank Jason Fowlkes for his assistance with operating and maintaining the LPX 300 laser, equipment setup, advice, and for sharing the results of his previous work. Won-Seok Kim assisted with solving problems encountered while performing experiments and locating vital equipment. I am also thankful to Dr. Anthony J. Pedraza for his continued scientific guidance, several SEM photomicrographs and, along with the Solid State Division of Oak Ridge National Laboratory, use of the Dektak II profilometer.

Greg Jones and Dr. Charlie R. Brooks are acknowledged for SEM training and troubleshooting.

Abstract

The formation of columnar morphologies in single-crystal Si by pulsed laser irradiation has been previously reported. This formation has occurred with multiple process atmospheres, pulse duration and number, and laser wavelengths. Few experiments have been performed in vacuum, and it is believed that examining the effect of fluence and pulse number on single-crystal Si irradiated in vacuum will further understanding of microcolumn nucleation and growth mechanisms. Samples were prepared using a 248-nm KrF excimer laser with a pulse duration of 25 ns and a pulse frequency of 10 Hz in a chamber evacuated to 10^{-4} torr. The average fluence and number of pulses were varied. Profilometry revealed that structure formation was more rapid in vacuum than in gaseous atmospheres and that the structures observed were taller, attaining heights greater than 40 μm . It was also noted that microcolumns formed only in a specific fluence range. Scanning electron microscopy (SEM) determined that, after the formation of periodic structures in the fluence range 3.9-5.0 J/cm², pits and erect columns form abruptly and concurrently followed by vertical and lateral propagation and possibly merger. It is hypothesized that columns are growing at least in part by redeposition of ablated material by the vapor-liquid-solid (VLS) mechanism in both vacuum and gaseous atmospheres.

TABLE OF CONTENTS

	PAGE
INTRODUCTION	1
Laser-induced surface modification of materials	1
Applications of black silicon	2
Microcolumn growth	4
EXPERIMENTAL PROCEDURE	8
Beam energy distribution	8
Sample preparation and processing	9
EXPERIMENTAL RESULTS	13
Profilometry	13
SEM photomicrography	19
DISCUSSION	26
LIPSS and nucleation and early growth of microcolumns	26
Mature morphology	30
CONCLUSIONS	33
FUTURE WORK	34
REFERENCES	35

LIST OF FIGURES

FIGURE	PAGE
1. Beam energy distribution	8
2. Experimental setup	9
3. Dektak II scans of specimens processed at $\langle\phi\rangle = 2.3 \text{ J/cm}^2$ in vacuum	14
4. Dektak II scans of specimens processed at $\langle\phi\rangle = 3.0 \text{ J/cm}^2$ in vacuum	15
5. Dektak II scans of specimens processed at $\langle\phi\rangle = 3.3 \text{ J/cm}^2$ in vacuum	16
6. Dektak II scans of specimens processed at $\langle\phi\rangle = 4.7 \text{ J/cm}^2$ in vacuum	17
7. Dektak II scans of specimens processed at $\langle\phi\rangle = 7.5 \text{ J/cm}^2$ in vacuum	18
8. Specimen processed in vacuum, $\langle\phi\rangle = 3.0 \text{ J/cm}^2$, $N = 2000$	19
9. Specimen processed in vacuum, $\langle\phi\rangle = 7.5 \text{ J/cm}^2$, $N = 50$	19
10. Specimens processed in vacuum at $\langle\phi\rangle = 7.5 \text{ J/cm}^2$ in vacuum	20
11. Specimens processed in vacuum at $\langle\phi\rangle = 7.5 \text{ J/cm}^2$ in vacuum	21
12. Specimen processed in vacuum. $\langle\phi\rangle = 7.5 \text{ J/cm}^2$, ϕ (local) $\approx 3.9 \text{ J/cm}^2$, $N=25$	22
13. Specimens processed in vacuum. $\langle\phi\rangle = 7.5 \text{ J/cm}^2$, ϕ (local) $\approx 5.0 \text{ J/cm}^2$, $N=25$	23
14. Specimen processed in vacuum, $\langle\phi\rangle = 4.1 \text{ J/cm}^2$, $N = 800$	24
15. Specimen processed in vacuum, $\langle\phi\rangle = 4.1 \text{ J/cm}^2$, $N = 800$, demonstrating cracking	25
16. (100) Si wafer irradiated in SF_6 , ϕ and N unknown.	28
17. Summary of microcolumn and tower formation mechanisms with increasing pulse number	32

NOMENCLATURE

E	Total energy incident on sample (J)
A	Total area irradiated by laser (cm ²)
$\langle\phi\rangle$	Average fluence (also <i>energy density</i>) ($= E/A$) (J/cm ²)
ϕ	Local fluence (J/cm ²)
λ	Laser wavelength (nm)
N	Number of pulses
P	Total chamber pressure (torr)
x	Horizontal direction parallel to beam
y	Horizontal direction perpendicular to beam
z	Vertical direction
a	Width of beam in y direction (cm)
b	Width of beam in z direction (cm)
PLD	<i>pulsed laser deposition</i>
VLS	<i>vapor-liquid-solid</i>
VS	<i>vapor-solid</i>
CVD	<i>chemical vapor deposition</i>
LIPSS	<i>laser-induced periodic surface structures</i>
SEM	<i>scanning electron microscopy</i>

INTRODUCTION

Laser-induced surface modification of materials

Surface modification of materials by laser irradiation is a relatively new field, having only emerged as a specialization within applied physics and materials science in the last three decades. Observation of damage in optical components led to controlled study of the effect of lasers on surfaces. The intensities possible with laser irradiation—up to 10^{18} W/m² (10^{15} times that of solar radiation at sea level) for some pulsed excimer lasers—create structures on surfaces that are unique and as a result have unique applications and properties. The effect of laser irradiation on polymers, superconducting oxides, metals, and other materials has been studied extensively and has given rise to entirely new processes such as laser welding, micromachining, and pulsed laser deposition (PLD).

The topographical changes due of laser irradiation on materials are described by Foltyn¹ and can be generalized as follows. At low numbers of pulses or low fluences above the melting threshold, laser-induced periodic surface structures (LIPSS) are formed. Commonly referred to as “ripples,” this topology resembles standing waves and is formed by resolidification of perturbations in liquid material melted during the pulse or by preferential material removal. Wave peaks can be points, ridges, or both. The period of the structure seems related to wavelength, but in the work detailed later the observed period of ripples was two orders of magnitude greater than the wavelength, making quantification difficult. At intermediate pulse numbers or fluences (typically between 1 and 6 J/cm² for thin-film PLD of semiconductors and wear-resistant coatings), the amplitude of the periodic structures can increase substantially. Such structures are usually described with the generic label “cones.” The formation of cones and

ripples seems to have a variety of causal mechanisms, but seem to have a universal quality² due to their presence in a variety of materials and original surface conditions. Most of these usually can be categorized as removal or expansion processes, although rough cones forming from redeposition of debris are sometimes seen in polymers.³ In removal processes preferential ablation occurs, usually attributed to some variation in chemistry due to preexisting impurities, reactions initiated by the laser (common in polymers), thermodynamically driven segregation, etc.

Rothenberg and Kelly⁴ coined the phrase “hydrodynamic sputtering” to describe a common type of expansion process, hypothetically driven by thermal expansion of molten protrusions in the direction of the beam. Expansion is checked by the increase in surface tension as the liquid cools by conduction into the substrate. Material is ejected in this range as plasma, gas, and even solid particles, but the ablation rate is considerably less than that seen at higher fluence.

It is in this range of fluence that periodic topology formation leads to the formation of whiskers or whisker-like structures, usually referred to as “microcolumns,” with increasing pulse number in irradiated specimens of single-crystal Si. As will be discussed below, there is uncertainty if this is a simple hydrodynamic process.

At very high values of fluence, the net rate of removal is so high that significant material is permanently lost, with a variety of topologies resulting on the surface in the path of the laser beam.

Applications of black silicon

Fine-tip microcolumns in Si have a variety of potential applications in photonic devices due to the extremely low reflectivity of microcolumn clusters. Almost all of the light striking a

region of microcolumns is absorbed by reflection between microcolumns. (This will be seen to be an essential aspect of their formation.) It is this property of near-total absorption which has led to the use of the term “black silicon” in the popular media⁵ to refer to formations of Si microcolumns. As would be expected from Kirchoff’s Law of blackbody radiation, the low reflectivity of black silicon implies a high emissivity.

The photoluminescence of atomically sharp whiskers, usually attributed to quantum confinement effects⁶, make them the morphology of choice for filaments in scanning probe devices. These are currently made from tungsten, but tungsten has many drawbacks, including the difficulty of maintaining ultrahigh purity, which is a prerequisite for field-emission tips. Si whiskers have been grown by chemical vapor deposition (CVD) for this application utilizing the vapor-liquid-solid (VLS) phenomenon, but this method requires Au impurities.⁷ Si microcolumns can be formed without doping and thus are promising for this application. It is important to note that in columns formed by either CVD or current laser irradiation techniques the resulting structures must be passivated and etched to obtain atomically sharp tips. This is because at present there has not been a successful demonstration of the growth of nanocolumns (columns with tip diameters on the order of 1 nm) in Si.

Another application of current interest for which a high-photoluminescence material is well-suited is that of flat-panel displays. Since virtually all of the power input would be emitted by black silicon, it is conceivable that it would be a highly efficient and bright material for displays. Little work has been done in this direction, however.

Perhaps the most promising direction for application of Si microcolumns is that of solar collectors. Low-reflectivity semiconductors are optimal for this application. Semiconductors

allow for ready conversion of solar energy into electrical current, but the chronic inefficiency of existing cell technologies might be addressed with black silicon.

Microcolumn growth

No complete model of the formation of microcolumns has been proposed that incorporates all observed features of growth. Considerable disagreement exists regarding the origin of several vital phenomena observed in the nucleation, growth, and termination of microcolumn structures. This is compounded by disagreement in terminology. Some confusion seems to exist in the literature about the distinction between “spikes,” “mushrooms,” and “columns,” so that proposals for responsible mechanisms do not comprehensively examine all relevant phenomena.

Sánchez *et al.* of the University of Barcelona have hypothesized that microcolumn phenomena, for which they also use the term “whiskerlike structures,” can be described in terms of thermocapillary flow of molten silicon, driven by the variation of surface tension with local temperature, and specifically state that neither recoil from material ejection⁸ nor preferential removal from the regions surrounding the microcolumn tips⁹ can significantly contribute to microcolumn formation. Their work has been performed exclusively in air with an ArF laser ($\lambda = 193$ nm), however, and has not examined the process in vacuum, He, Cl₂, or SF₆¹⁰ or at other excimer wavelengths. It should be noted that the topology reported in Figure 3 of Sánchez *et al.*¹¹ are dramatically different from those previously prepared by Fowlkes¹² with a KrF laser ($\lambda = 248$ nm) in air. In this figure, the deep pits almost always seen in Fowlkes’s work are absent, and only shallow depressions are formed; additionally, though the microcolumns are whisker-like with straight shafts and small tips, the bases are wide, indicating a continuous transition

from ridges to microcolumns. Sánchez *et al.* also report “mushrooms,” very large-tipped and short structures which do not propagate toward the incident beam.¹³

Another limited description of the formation of microcolumns is given by Mazur *et al.* of Harvard University. In specimens processed in SF₆ and Cl₂ with a Ti:sapphire laser ($\lambda = 800$ nm) with 100-fs pulses at $\phi = 10$ J/cm², sharp columns with round tips are reported.¹⁴ It is important to note that mature structures similar to those reported later in this work were also observed in Si processed in vacuum, but the authors reserve the use of the term “columns” for sharp structures such as those seen in reactive atmospheres. Vacuum structures are referred to as “blunt spikes,” and the authors cite von Allmen and Lau’s model for the formation of the structures in vacuum.¹⁵ In this model, the spikes form from variable recrystallization rates in different regions of supercooled liquid protrusions.

A detailed mechanism is not proposed, merely that “chemical reaction between SF₆ or Cl₂ and silicon contributes to the formation of the sharp spikes.”¹⁶ However, the *Scientific American* article contains an inaccurate statement: “When [Mazur *et al.*] similar experiments with nitrogen and helium, the surface became textured but no spikes formed.”¹⁷ This is in contradiction to Her *et al.*’s previously published results.

An additional hypothesized factor in microcolumn formation is analogous to the VLS mechanism of whisker growth summarized by Givargizov.¹⁸ In conventional VLS growth, a vapor supersaturated with the desired material condenses preferentially on liquid due to the abundance of deposition sites on the rough liquid surface. The concentration gradient between the liquid-vapor interface and the solid-liquid interface drives diffusion of condensates toward the solid-liquid interface. An impurity that has a sharp eutectic with the desired material is present as a solute, and the increase in solvent concentration creates constitutional supercooling,

solidification, and migration of solute upward. If the surface tension of different crystallographic planes with liquid is anisotropic, solidification will be unidirectional.

Pedraza *et al.* use the term “catalyst-free” VLS growth¹⁹ to describe a proposed process similar to conventional VLS growth as described above. In this model, a molten tip is formed which serves the same role of accommodation as the liquid in conventional VLS. Particles of ablated material adhere preferentially to this molten tip, feeding the liquid phase while the large thermal gradients present in laser processing drive resolidification at the solid-liquid interface.

This hypothesis is motivated in part by the observation that very deep pits often form during irradiation, apparently beginning from the depressed regions in LIPSS, in all processing atmospheres. It is known that pits serve to concentrate laser energy by trapping multiple reflections within the pit walls.²⁰ The laser intensity at the bottom of the pits is therefore extremely high, and it is almost certainly too high for liquid to survive in very deep pits. This casts doubt on the hypothesis that hydrodynamic flow can be responsible for all stages, especially later ones, of microcolumn growth.

The Laser Processing Laboratory at the University of Tennessee at Knoxville (UTK) has worked toward cataloging the effects of irradiating (100)-oriented single-crystal Si with a KrF excimer pulsed laser ($\lambda = 248$ nm). This has been performed in SF₆, air (82% N₂, 18% O₂), reduced-oxygen air (95% N₂, 5% O₂), 100% O₂, and to a limited extent Si₂H₆ and He. The aim of this experimental work has been to gather as much information as possible in an attempt to formulate a more comprehensive model of growth. Processing in different atmospheres permits the observation of the effects of different chemical systems on nucleation and growth, and varying fluence and pulse number allows for better understanding of process kinetics.

The work presented in this thesis focuses on determining, as completely as possible, the effects of different process times and fluences in another specific atmosphere, namely that of moderate vacuum ($\sim 10^{-4}$ torr). Preliminary studies did not indicate any variation in resulting microcolumn morphology or dimensions with lower pressures. It is expected that studying the changes in topology as the number of pulses increases at different fluences will give insight into growth mechanisms. Since there is no volatile gas in vacuum to react with Si, material removal by etching will not occur, nor can there be any chemical contribution to structure formation. For this reason, this work will examine the resulting structures with the aim of determining their similarity to previously observed “true” microcolumn morphology.

EXPERIMENTAL PROCEDURE

This work was performed with a Lambda Physik LPX 300 pulsed laser utilizing KrF excimer radiation ($\lambda = 248$ nm).

Beam energy distribution

The first step in this work was determination of the configuration of the beam, since it is known that the energy of excimer beams is heterogeneously distributed across the beam cross-section. For this determination a square slit was constructed with an area of ~ 0.1 cm² on a frame so that the slit could be moved in both the y and z directions. A power meter placed behind the slit would give the energy incident on the slit. The fluence distribution was found to be

$$\phi(y, z) = 2.1 \langle \phi \rangle \left(102.1 \left| \frac{y}{a} \right|^4 - 102.1 \left| \frac{y}{a} \right|^3 + 25.283 \left| \frac{y}{a} \right|^2 - 1.8788 \left| \frac{y}{a} \right| + 1.0269 \right) \left(-3.714 \left| \frac{z}{b} \right|^2 - 0.143 \left| \frac{z}{b} \right| + 0.9706 \right) \quad (1)$$

using polynomial regression. The distribution is graphically illustrated in Figure 1.

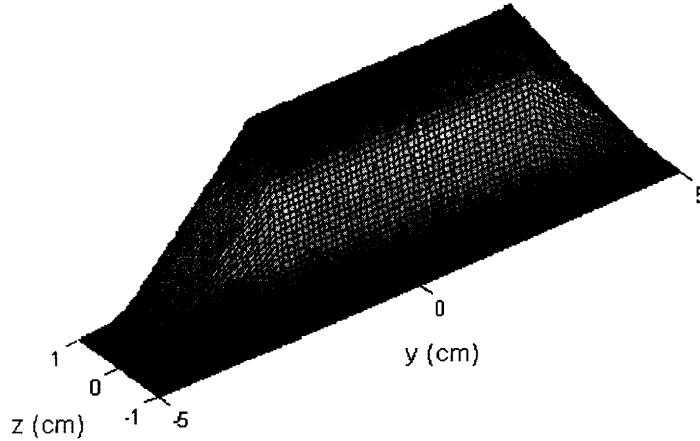


FIG. 1. Beam energy distribution. Note that a “plateau” exists in the center where the fluence is near maximum.

Although the actual distribution on the target would vary with small changes in optical alignment, this equation allows estimation of the fluence at any spot on an observed specimen.

Sample preparation and processing

Single-crystal Si wafers with a (100) orientation and one polished surface were used for all tests. Due to the wafers' brittleness, they were easily cut to a variety of shapes using a scribe.

Undesirable oxide layers form on wafers stored in air so, prior to processing, each specimen was placed in a bath containing HF with an approximate concentration of 4.5 mol/L for 30 s. The specimen was then removed, rinsed in distilled water followed by methanol, and blown dry with a mixture of 96% Ar and 4% H₂. The specimen was placed on the sample holder with silver paint so that the incident beam would fall upon the polished surface. The holder was then placed in the chamber and pumping began immediately. The rotary pump was used to evacuate the chamber to 10⁻³ torr, and the turbomolecular pump finished pumping to 10⁻⁴ torr.

Processing samples in vacuum presented two significant difficulties. Initially, double-sided transparent adhesive tape with paper insulation between the tape and the metal holder was used, but this proved impractical as the heating during irradiation in vacuum was sufficient to cause the tape adhesive to decompose. This was solved by using silver paint to attach the specimens. Also, without an interfering medium, some of the Si ejected during irradiation was deposited on the silica window through which the beam entered. Cleaning the windows was difficult, so the window was moved several centimeters forward by extending the chamber with a tapered nipple. The plume of material then struck the chamber wall instead of the window. Figure 2 shows the experimental setup used in these tests. The modified chamber is shown. Note that the sample holder was tilted 5° from the laser beam so that the reflected laser light would not travel back through the optics and cause damage.

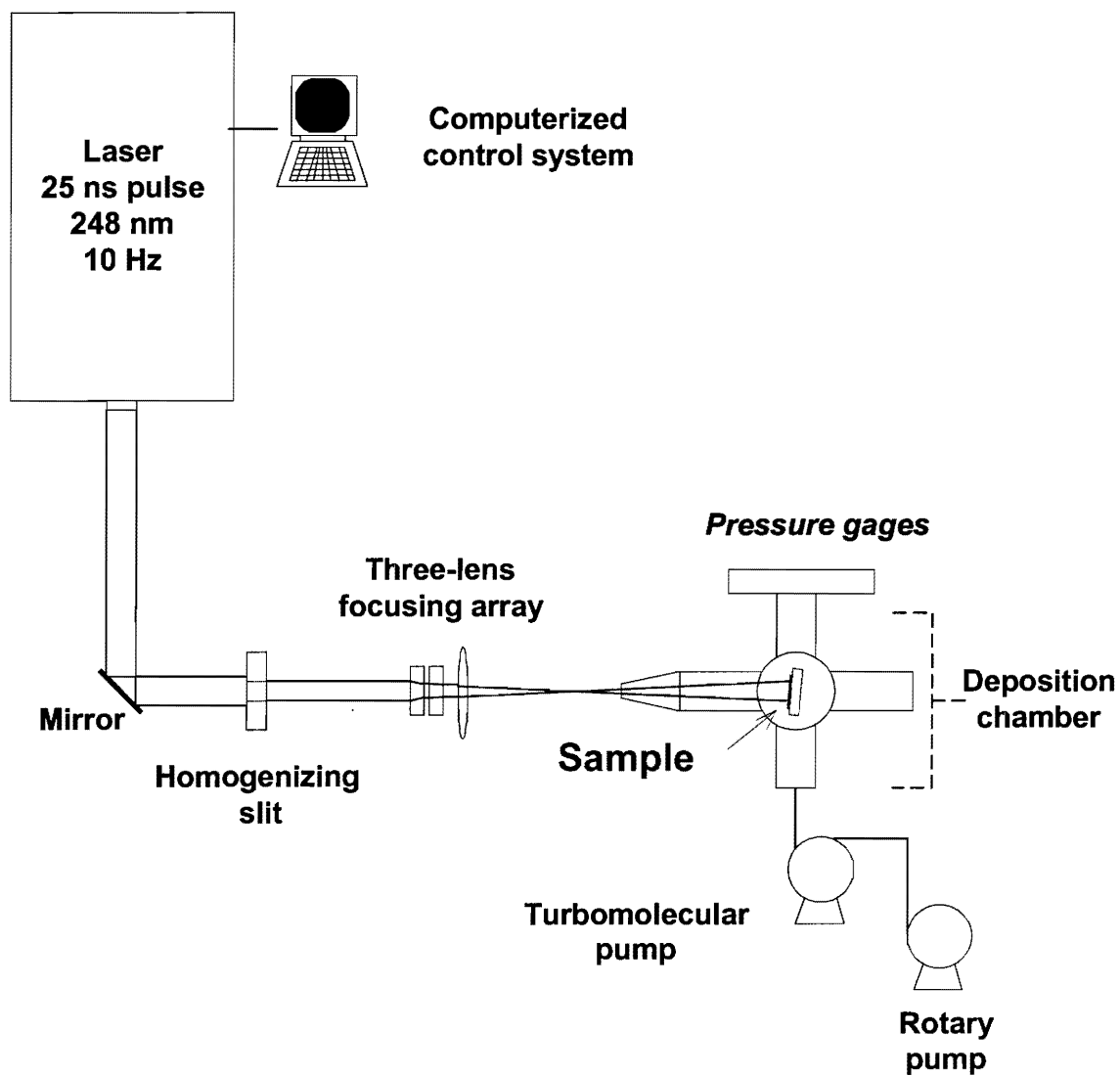


FIG. 2. Experimental setup.

The throughput energy of the laser was held constant for each batch of samples. Depending on the age of the fill, E ranged from 220 mJ to 280 mJ. Energy can be controlled by varying the high voltage setting of the LPX 300, but this is unadvisable since the energy varies from pulse to pulse as high voltage decreases below ~ 21 kV. Thus, the highest setting (23.0 kV) was typically used. E was measured by a power meter before and during the processing of each sample batch.

The area of the beam was varied by moving the lens array in the x direction to change the area of the beam incident on the target. It was discovered early in the work that the focal point of the laser beam should be between the lens array and the target, *i.e.* the diverging beam should be used. This was necessary due to the extremely poor beam distribution resulting from using the convergent beam.

An additional difficulty encountered in processing was that the area A irradiated by the beam could not be accurately measured without examining the specimen by SEM after irradiation. Due to the heterogeneous incoming beam, a much lower fluence impinges on the area at the fringe of the beam than at the center. As a result, the burn paper used to verify optics alignment does show the complete area irradiated by the beam. Also, the area at the fringe on the Si targets is modified so slowly that most of the damage is below the surface at the edge and thus only visible in an SEM, which detects electrons scattered from below the surface. The beam print shows up as a dark area when examined by SEM.

Because of this uncertainty in A , two values of $\langle\phi\rangle$ are given. The estimated value refers to the average fluence measured using the area completely burned away by the laser in burn paper prior to processing. The actual value of average fluence was calculated from the area observed by SEM after processing and the recorded value of E . Table 1 summarizes the

specimens processed. It should be noted that all samples were processed with a chamber pressure of $P = 10^{-4}$ torr, a pulse duration of 25 ns, and a pulse frequency of 10 Hz. Henceforth, “ $\langle\phi\rangle$ ” will refer to the actual average fluence.

TABLE 1. Processed specimens.

Estimated $\langle\phi\rangle$	Actual $\langle\phi\rangle$	N
2.7 J/cm ²	2.3 J/cm ²	200
		400
		600
		800
		1000
		2000
3.6 J/cm ²	3.0 J/cm ²	1000
		2000
3.8 J/cm ²	3.3 J/cm ²	200
		400
		600
		800
		1000
		2000
4.7 J/cm ²	4.1 J/cm ²	200
		400
		600
		800
		1000
		2000
4.1 J/cm ²	7.5 J/cm ²	10
		25
		50
		100

EXPERIMENTAL RESULTS

Profilometry

Processed specimens were examined by a Dektak II profilometer at Oak Ridge National Laboratory. The profilometer probe travels in a line across the sample surface and measures the detected elevation of points along the line. The height or depth of the sample from the original surface is then plotted as a function of distance traveled.

Scans were made along the vertical line of symmetry of the beam-modified region, *i.e.* in the z direction with $y \approx 0$. The results are demonstrated in Figures 3-7. It should be noticed that scans were not available for all specimens, and that the scale on both the abscissa and ordinate of the scans varies from plot to plot.

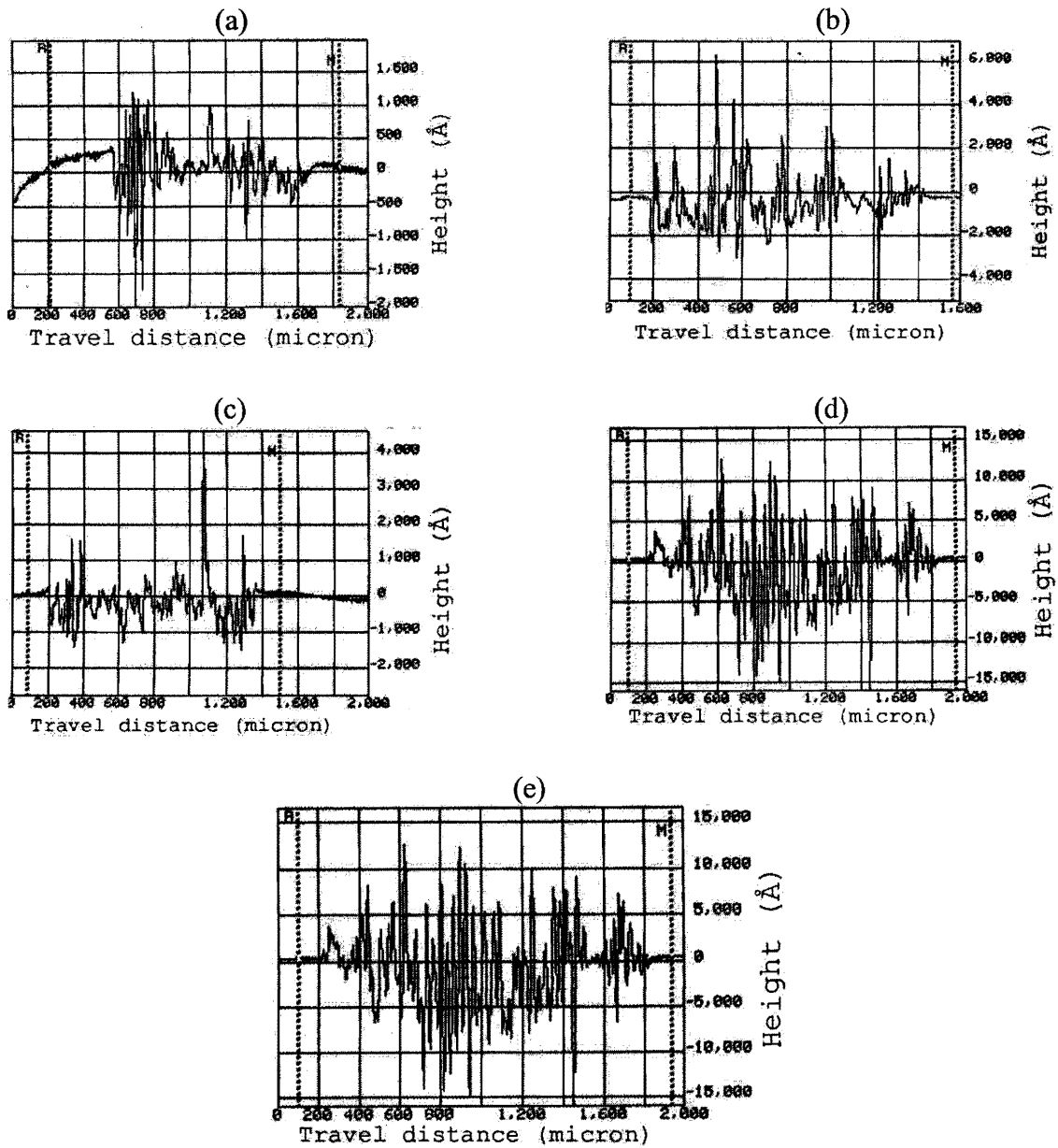


FIG. 3. Dektak II scans of specimens processed at $\langle \phi \rangle = 2.3 \text{ J/cm}^2$ in vacuum. (a) $N = 400$. (b) $N = 600$. (c) $N = 800$. (d) $N = 1000$. (e) $N = 2000$.

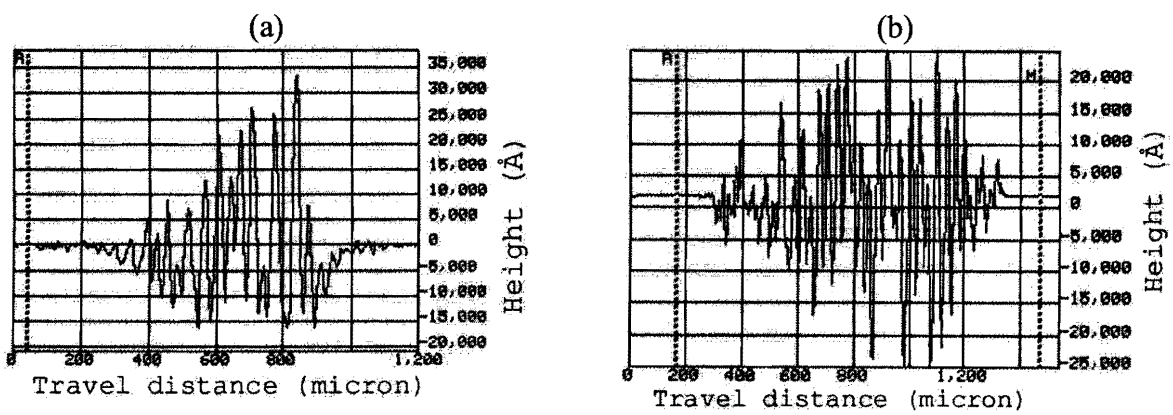


FIG. 4. Dektak II scans of specimens processed at $\langle \phi \rangle = 3.0 \text{ J/cm}^2$ in vacuum. (a) $N = 1000$. (b) $N = 2000$.

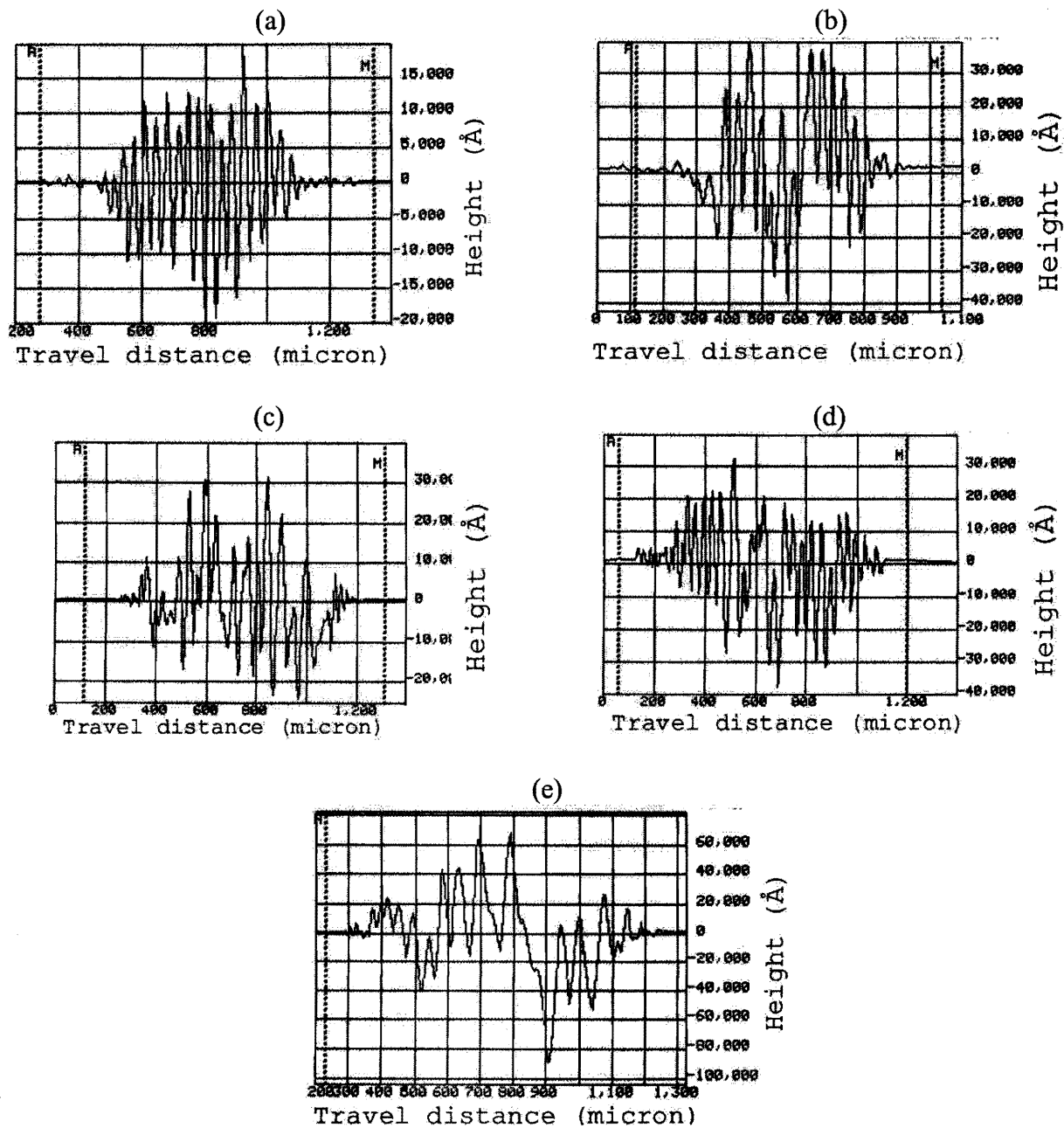


FIG. 5. Dektak II scans of specimens processed at $\langle \phi \rangle = 3.3 \text{ J/cm}^2$ in vacuum. (a) $N=400$. (b) $N=600$. (c) $N=800$. (d) $N=1000$. (e) $N=2000$.

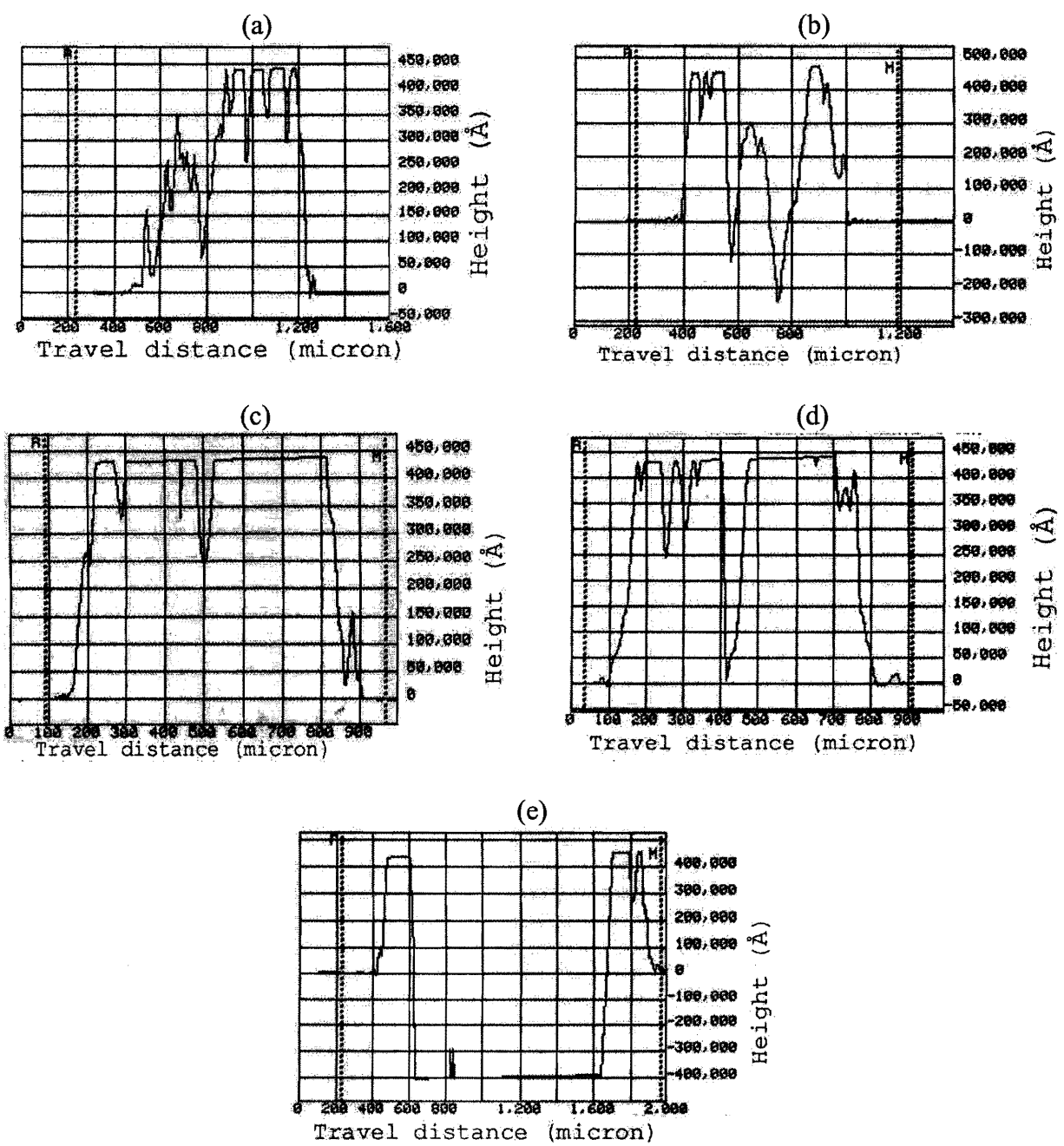


FIG. 6. Dektak II scans of specimens processed at $\langle \phi \rangle = 4.7 \text{ J/cm}^2$ in vacuum. (a) $N=200$. (b) $N=400$. (c) $N=600$. (d) $N=800$. (e) $N=2000$.

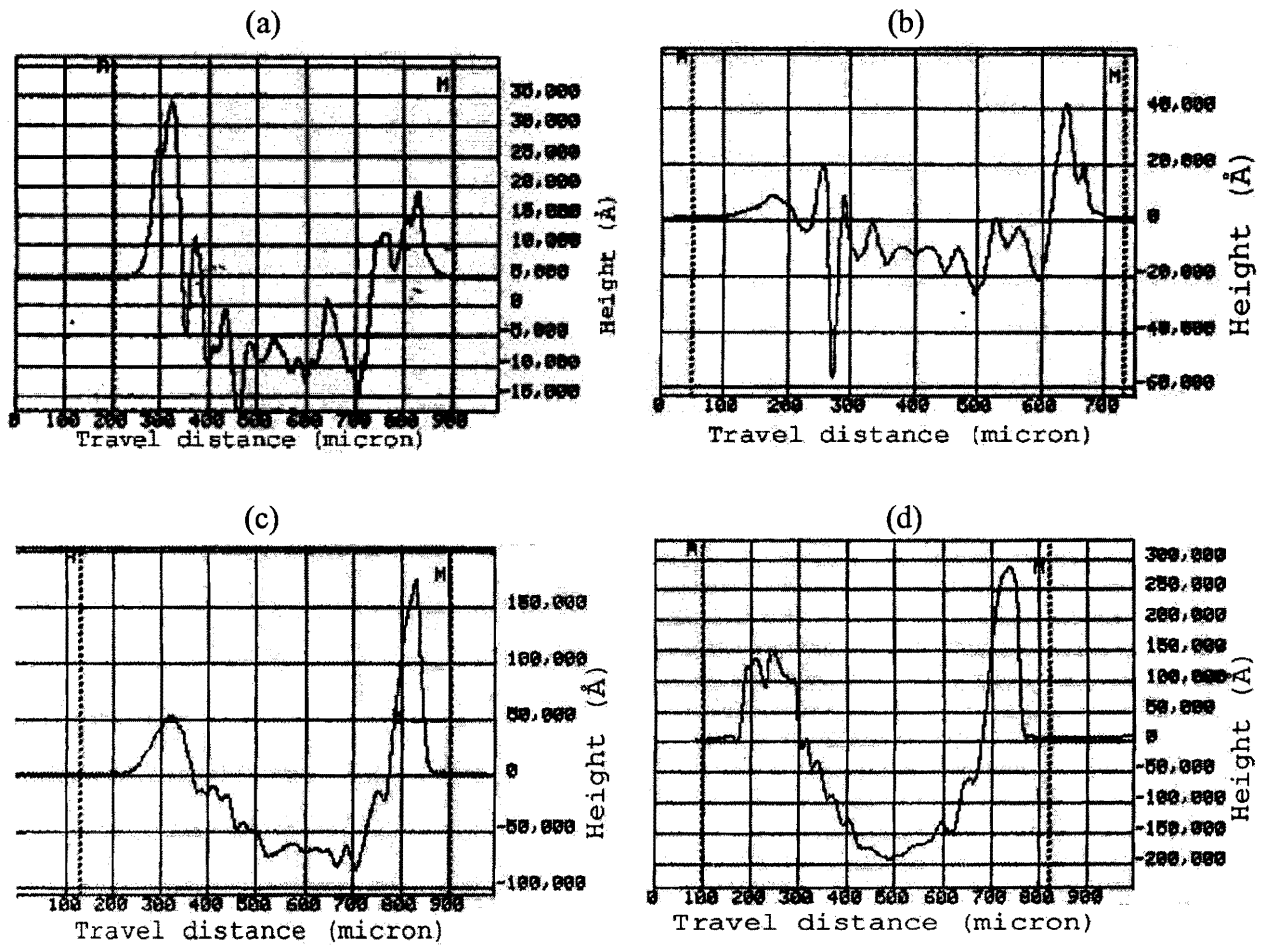


FIG. 7. Dektak II scans of specimens processed at $\langle \phi \rangle = 7.5 \text{ J/cm}^2$ in vacuum. (a) $N=10$. (b) $N=25$. (c) $N=50$. (d) $N=100$.

SEM photomicrography

Specimens were also examined using a Cambridge Stereoscan 360 scanning electron microscope. All specimens were photographed using secondary electrons.

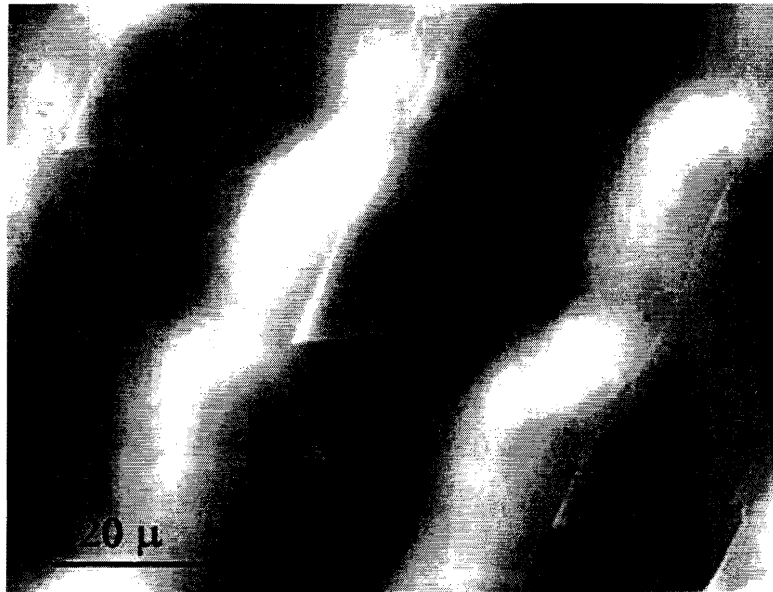


FIG. 8. Specimen processed in vacuum. $\langle\phi\rangle = 3.0 \text{ J/cm}^2$, $N = 2000$.



FIG. 9. Specimen processed in vacuum. $\langle\phi\rangle = 7.5 \text{ J/cm}^2$, $N = 50$.

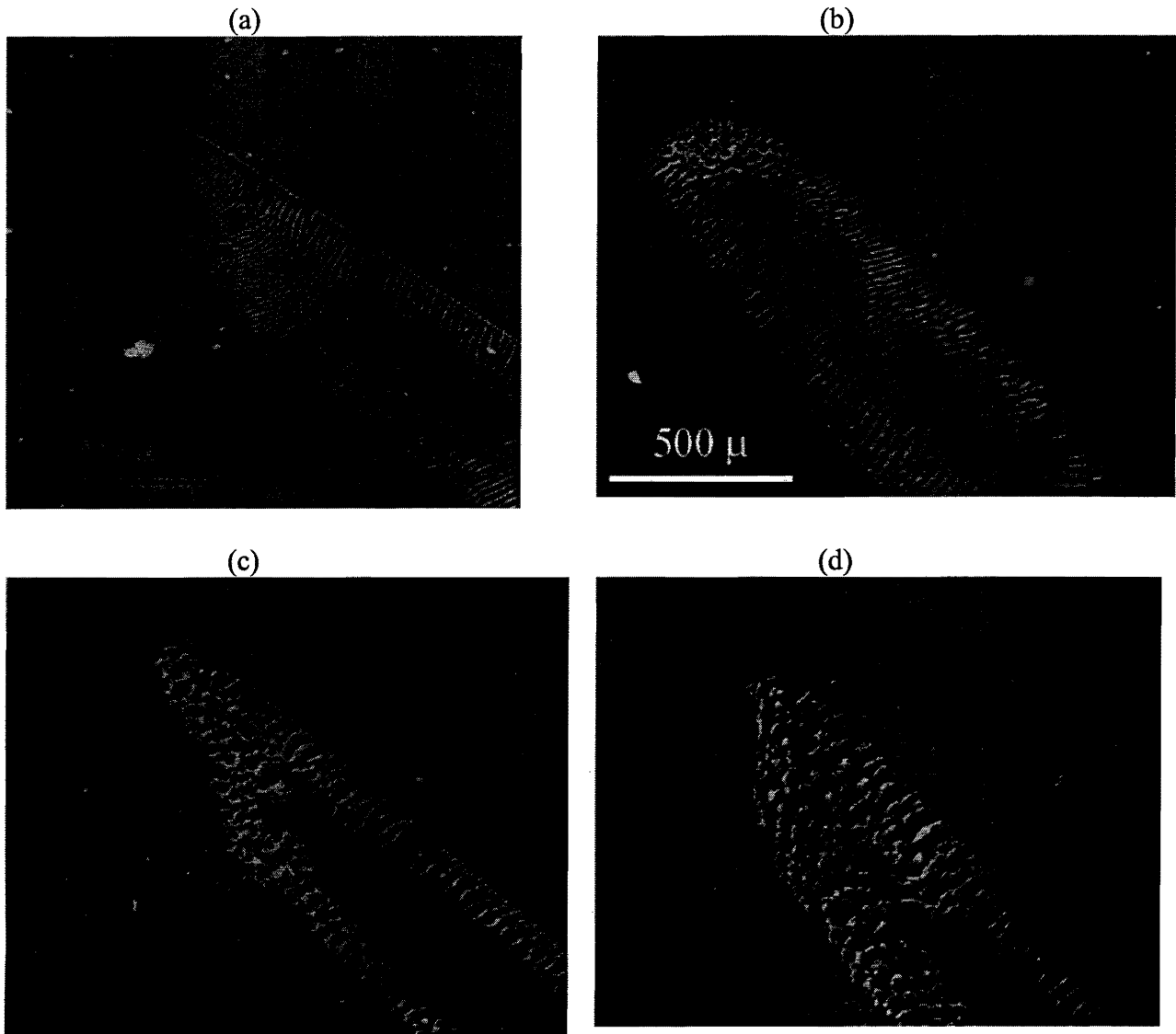


FIG. 10. Specimens processed at $\langle \phi \rangle = 7.5 \text{ J/cm}^2$. (a) $N = 10$. (b) $N = 25$, other end of beam. (c) $N = 50$. (d) $N = 100$.

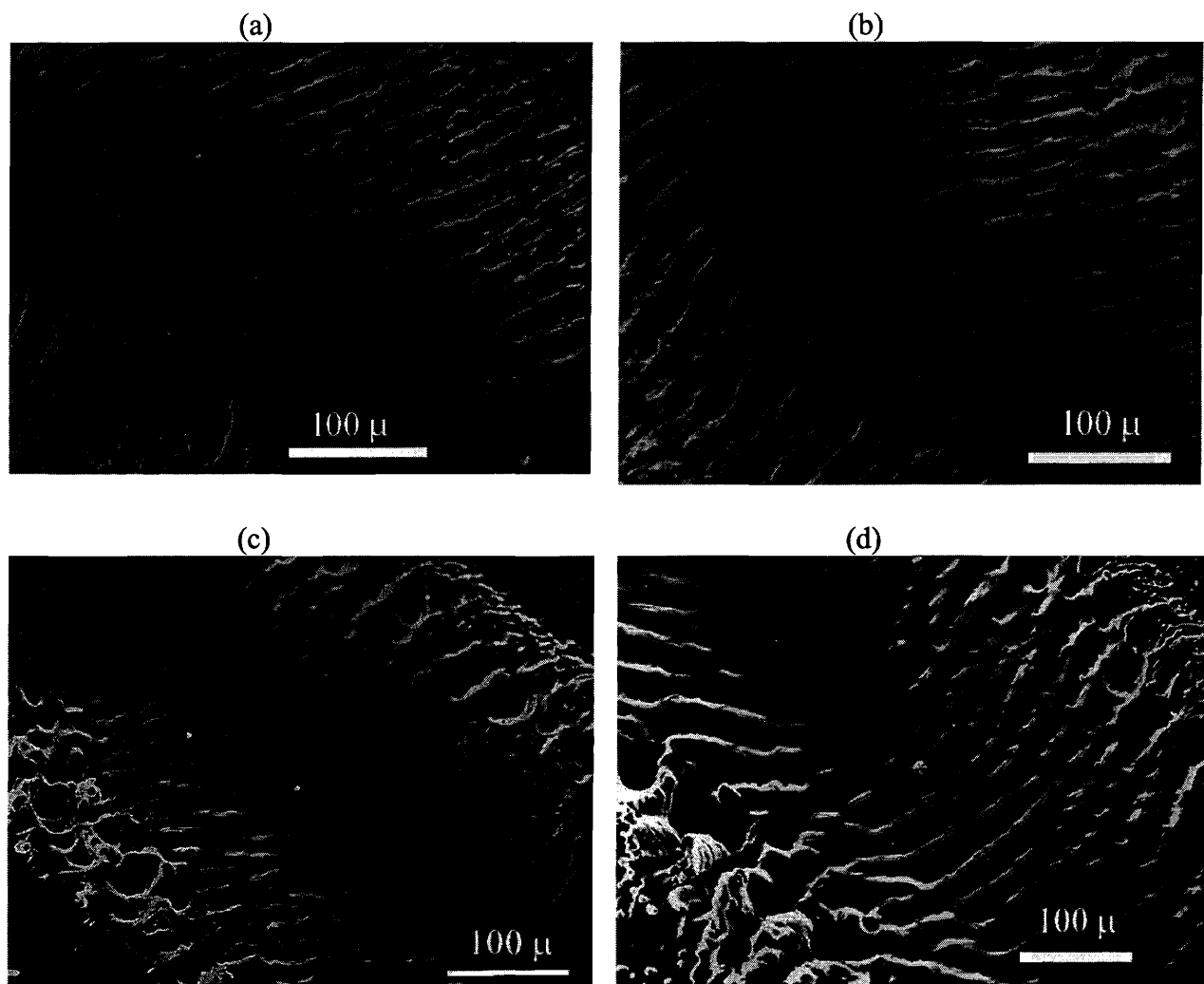


FIG. 11. Specimens processed at $\langle \phi \rangle = 7.5 \text{ J/cm}^2$ in vacuum. (a) $N = 10$. (b) $N = 25$. (c) $N = 50$. (d) $N = 100$.

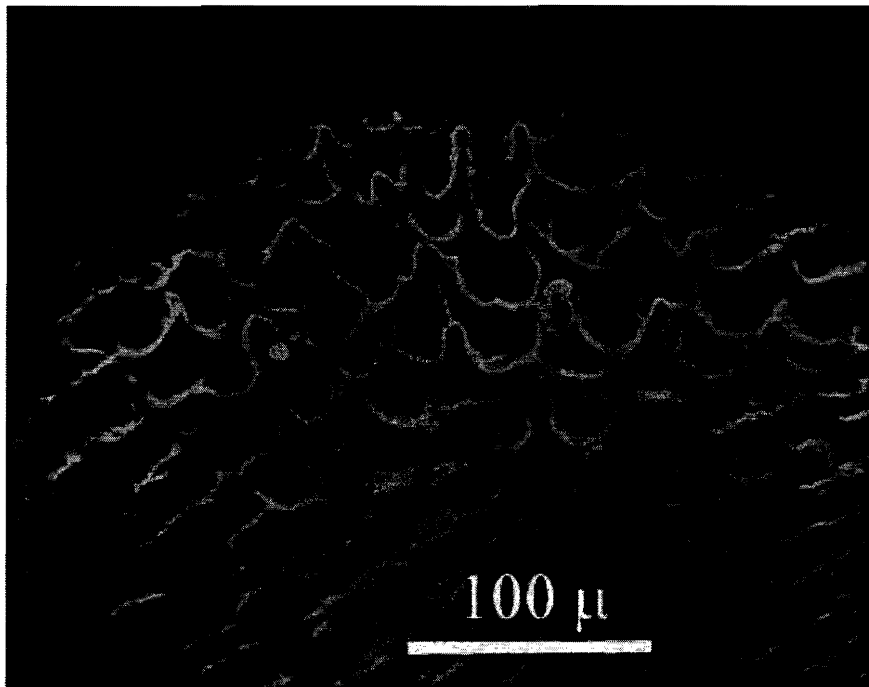


FIG. 12. Specimen processed in vacuum. $\langle\phi\rangle = 7.5 \text{ J/cm}^2$, ϕ (local) $\approx 3.9 \text{ J/cm}^2$, $N = 25$.

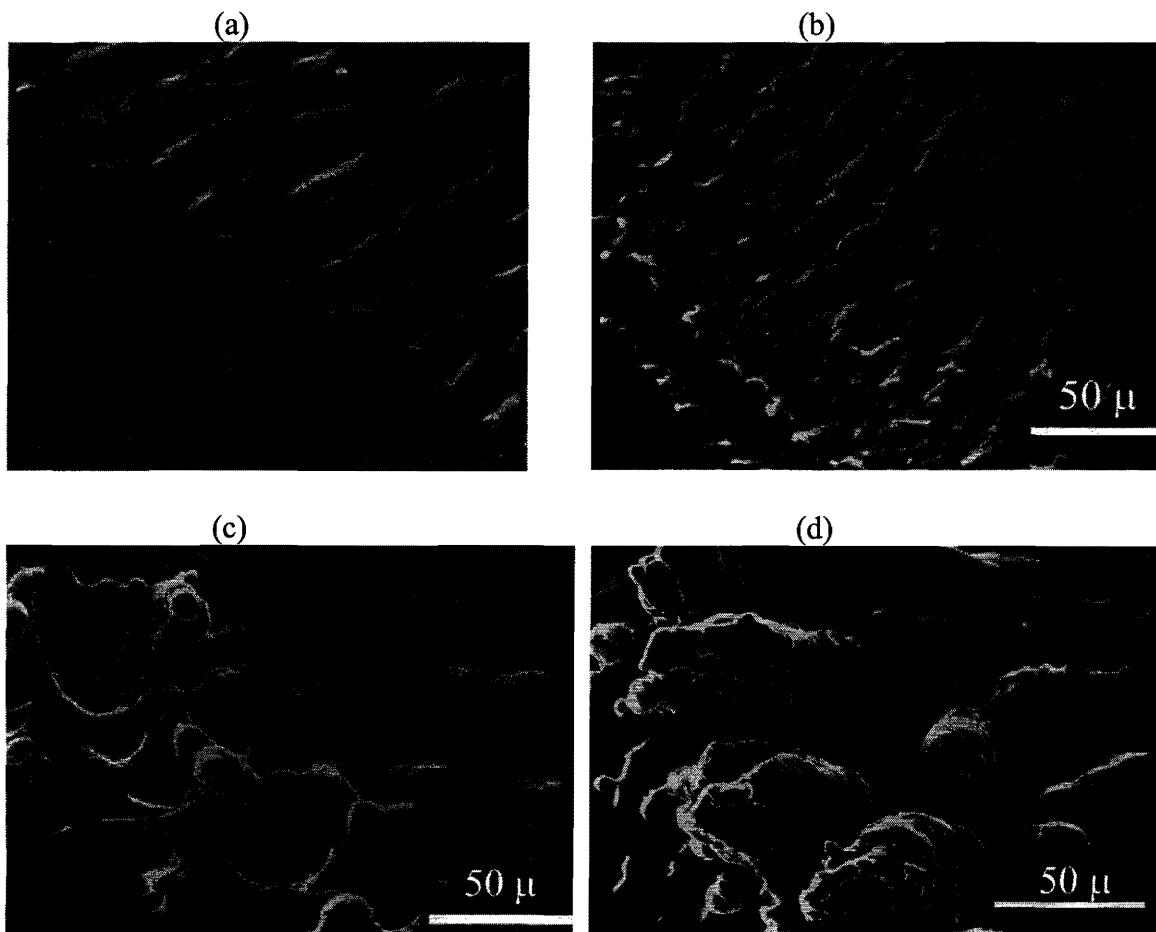


FIG. 13. Specimens processed in vacuum. $\langle\phi\rangle = 7.5 \text{ J/cm}^2$, $\phi (\text{local}) \approx 5.0 \text{ J/cm}^2$. (a) $N = 10$. (b) $N = 25$. (c) $N = 50$. (d) $N = 100$.

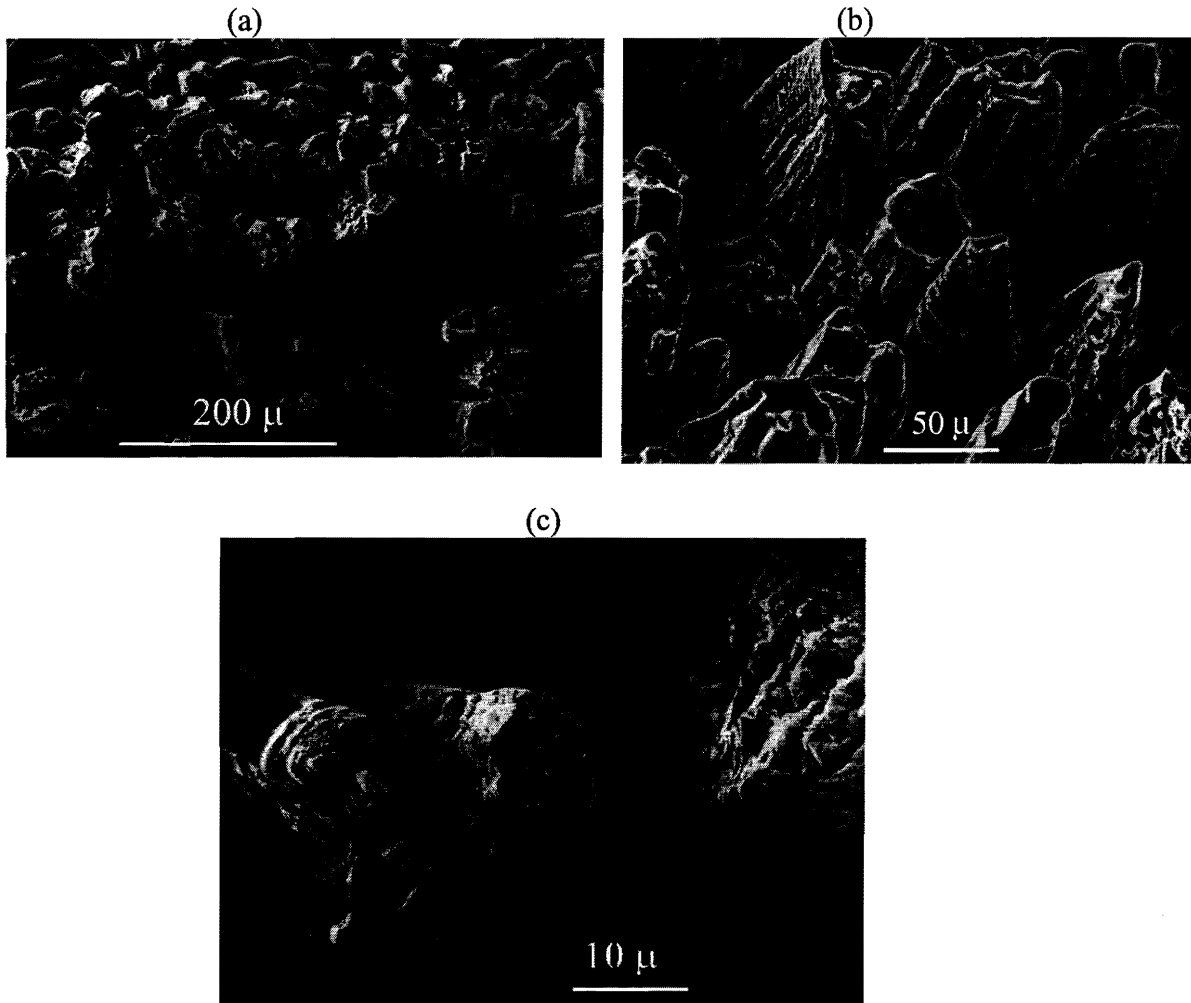


FIG. 14. Specimen processed in vacuum, $\langle\phi\rangle = 4.1 \text{ J/cm}^2$, $N = 800$.

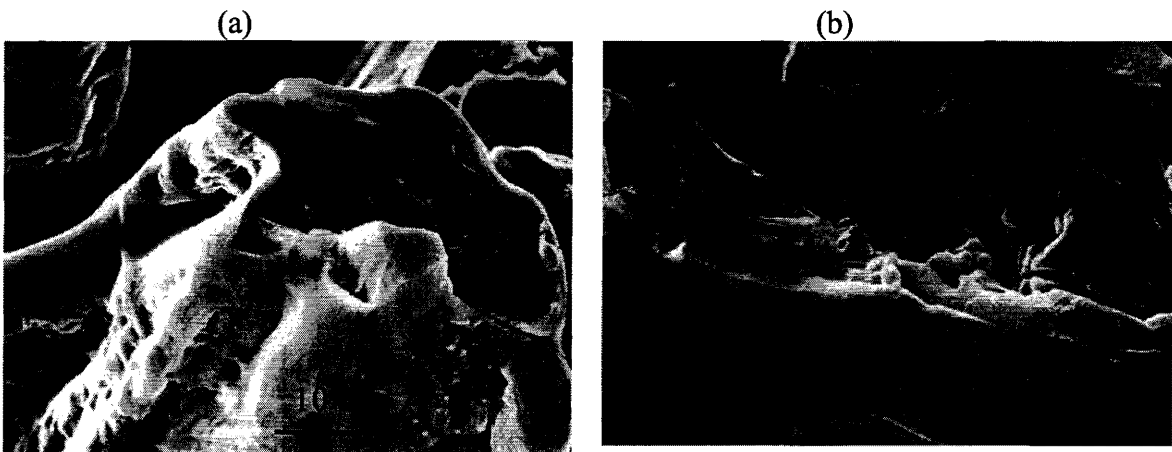


FIG. 15. Specimen processed in vacuum, $\langle\phi\rangle = 4.1 \text{ J/cm}^2$, $N = 800$, demonstrating cracking.

DISCUSSION

LIPSS and nucleation and early growth of microcolumns

From the profilometer scans in Figures 3, 4, and 5 an oscillatory pattern is observed, increasing in amplitude with both N and $\langle\phi\rangle$. Figure 8 shows ripples at $\langle\phi\rangle = 3.0 \text{ J/cm}^2$ and $N = 2000$, where the ripples have an amplitude of $2 \text{ }\mu\text{m}$ (see Figure 4b). It appears that conical structures will not form at a fluence of 3.3 J/cm^2 or lower, but that LIPSS will form and increase in size. In Figure 5e, the amplitude of LIPSS is $6 \text{ }\mu\text{m}$, the largest observed. Periodicity does not appear to vary with the number of pulses.

The fact that the amplitude increases monotonically is indication that resolidification completes between pulses and that total remelting does not occur during a pulse. If this occurred, the amplitude would be relatively constant from pulse to pulse and taller structures could not form. Previous theoretical and experimental work by Singh and Narayan demonstrates that melt depths are less than $1 \text{ }\mu\text{m}$ and that complete resolidification occurs within 400 ns after pulse initiation.²¹ (Compare this to the 10^8 ns between pulses.) Though this work was performed with a XeCl laser ($\lambda = 308 \text{ nm}$), the values for KrF irradiation should not be significantly greater since ablation occurs through thermal and not optical absorption in most materials (with the notable exception of ceramic materials).

The specimens processed at $\langle\phi\rangle = 7.5 \text{ J/cm}^2$ give a rich description of topological evolution during irradiation due to the marked heterogeneity of the modified region, as may be observed in Figure 9. Using Equation 1 allows estimation of local fluence for the regions examined in Figures 12 and 13. Note that there is a central area for which ablation is higher; comparison with Figure 1 supports use of this estimate.

Figure 10 allows examination of the different phenomena observed. In the center region of the beam, where fluence is highest ($\phi > 10 \text{ J/cm}^2$), the ablation rate seems to greatly exceed the redeposition rate. Ridges are visible, but other structures never develop. Figure 7d shows that, at $N = 100$, the center has been ablated to a depth $20 \mu\text{m}$ below the original surface. This is less than the approximately $40 \mu\text{m}$ predicted by Shinn *et al.*,²² but since the fluence varies across the sample and the local fluences are not exactly known for the profilometer scans, this is not felt to be significant.

The outermost region ($0.4a < |y| \leq 0.5a$) is noticed to darken as N increases. At $N = 100$, the formation of LIPSS in this area can be observed.

Other regions show a marked increase in elevation. These are the regions where sharp ridges appear to give way to the growth of spikes. The topological change between $N = 25$ and $N = 50$ is dramatic and corresponds to the formation of columnar structures as seen in Figure 10c. The maximum elevation increases from $4 \mu\text{m}$ to $15 \mu\text{m}$ during this time (Figures 7b and 7c).

Structures with the microcolumn morphology have definitely formed at $N = 25$ where the local fluence is approximately 3.9 J/cm^2 . The abrupt departure from ridges, initiation of deep pits, and erect columns are very similar to features observed in Si irradiated in an SF_6 atmosphere, as seen in Figure 16. This specimen was processed in previous work performed in the UTK Laser Processing Laboratory.

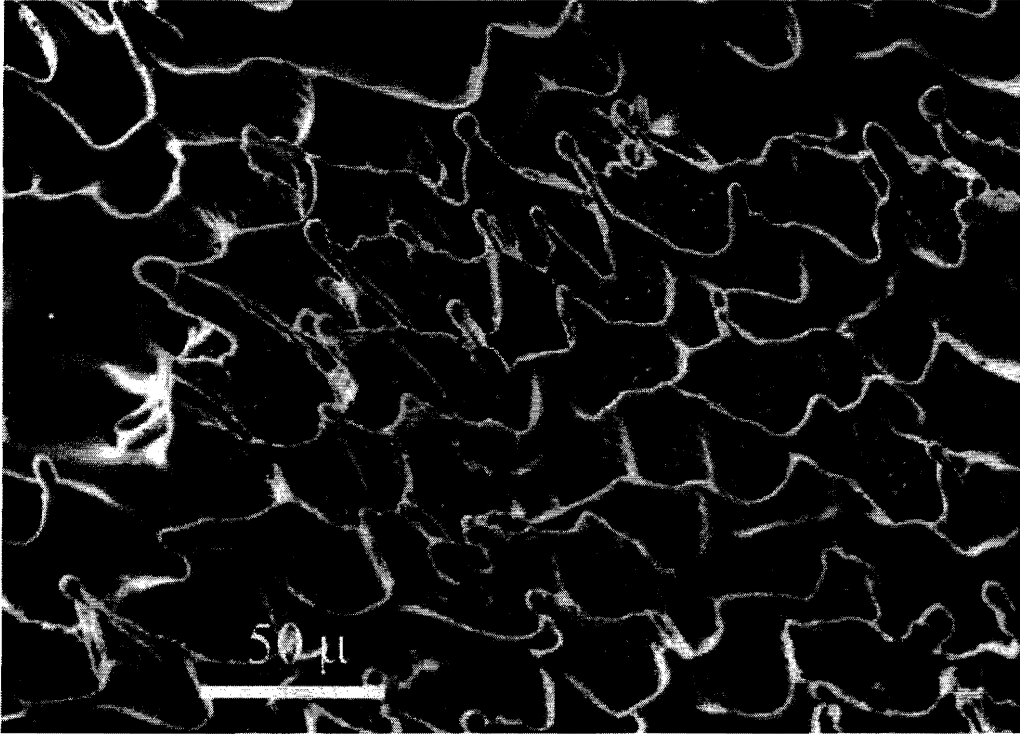


FIG. 16. (100) Si wafer irradiated in SF_6 , ϕ and N unknown.

The remarkable similarity between Figures 12 and 16 suggests that similar mechanisms are responsible for microcolumn nucleation and early growth stages in both vacuum and SF_6 .

Figure 13 shows a similar topological evolution with very rough microcolumns having emerged by fifty pulses (Figure 13c). Here also the formation of deep grooves and pits are precursors to microcolumn nucleation. Cracks forming at the edge are noticed, with an additional crack having formed between ten and twenty-five pulses. These cracks probably result from local stress generated by thermal cycling as material melts, flows, and resolidifies, with accompanying contraction and expansion and seem to be a site for early pit formation.

It is important to note that “liquid-like” globules can be seen on the top of columns, which is an indication of VLS behavior according to Givargizov.²³ Importantly,

these globules have also formed on the sides of columns by $N = 100$ (Figures 10d and 13d). This suggests that the VLS mechanism may play a major role in lateral propagation as well.

Figures 13c and 11c appear to give evidence that microcolumns which formed at $25 \leq N < 50$ continue to propagate in a similar manner. The surface is much rougher, however, than microcolumns formed in reactive processing atmospheres. In these other atmospheres chemical reactions occur between gases and Si, forming volatile intermediate products such as silicon oxides and fluorides on microcolumn surfaces. It is believed that the decomposition of these compounds when irradiated by the incident laser beam serves to remove material more efficiently than simple ablation. This erosion would occur where the beam is incident on the microcolumns, namely on the top and on the sides. This may explain why microcolumns grown in SF_6 and O_2 are less “sloppy” and perhaps even why they are shorter; the beam could be removing Si compounds not directly shielded from the beam.

A progression from the microcolumns in Figure 13c to the blocky structures in Figure 13d to the mature morphology in Figure 14 ($\langle \phi \rangle = 4.1 \text{ J/cm}^2$, $N = 800$) by the VLS mechanism in each instance does not appear inconsistent with the observed morphology. It is difficult to envision these rough surfaces forming by liquid flow, although an extremely nonuniform temperature distribution cannot be entirely discounted. The presence of shorter and rounder structures at the top and bottom of Figure 14a neighboring the larger “towers” is worth noting and seems to further indicate a direct transition from microcolumns to tower-like structures. These structures are approximately $3 \mu\text{m}$ tall (Figure 6d) at $N = 800$ and grow to $\geq 40 \mu\text{m}$ by two thousand pulses (Figure 6e). This is

consistent with the growth from 4 μm to 15 μm in Figures 7b and 7c that has been observed to be microcolumn growth by SEM (see above). Therefore, it is likely that the tower structures (referred to as “blunt spikes” by Her *et al.*²⁴) are formed from microcolumns (or are in fact large microcolumns), although it seems very likely that multiple columns may be merging to form towers and that each tower could be growing from multiple droplets. It should be noted that the spacing between structures has increased from Figure 10c ($N = 50$) to Figure 10d ($N = 100$) and that numerous droplets are closely grouped in Figure 13d.

Prior to examination of the low- N samples, it was thought that perhaps epitaxial deposition directly from the gas phase onto the solid (a VS mechanism) could produce more rapid growth, explaining the extreme height of the towers ($> 40 \mu\text{m}$). Although a very high supersaturation could result in redeposited material occupying of all available liquid sites and the redeposition of the surplus onto the solid, perhaps explaining the unusual morphology to some extent, this seems unnecessary in light of the apparent abundance of irregularly placed globules in the specimens processed at $N = 50$ and $N = 100$.

Mature morphology

The structures formed in vacuum are considerably taller than those formed in other atmospheres, including inert atmospheres such as He. The shorter structures formed in He could result from plasma shielding; the chamber pressure could constrain the plasma to the vicinity of the wafer surface, absorbing some of the incoming laser energy. Direct observation would be required to experimentally verify this conjecture. However, it is

clear that higher intensities produce larger structures, perhaps by either increasing the supersaturation in the vicinity of the surface, stimulating liquid flow, or both. It is also conceivable that gas or plasma pressure mechanically resists upward propagation of structures.

It is unclear why column growth terminates at a given height or why mature towers are subsequently ablated followed by growth of the structures neighboring the sites of the former towers, giving the appearance of outward migration. It is possible that at some point the structures reach the plasma, the index of refraction of the plasma shifts so that it becomes opaque, or that shockwaves emanating from the plasma disrupt the activity of the liquid. Cracks are noted in towers in Figure 15. It was originally presumed that this resulted from handling damage after processing, but this is not consistent with the presence of cleavage inside the tower. It is noteworthy that Sánchez *et al.* also observed cracks in specimens irradiated in air and also speculated that handling was responsible. They also concluded that some aspect of processing, probably shockwaves in the plasma, caused the damage.²⁵

Figure 17 summarizes the sequence of events seen in the samples processed at $\langle\phi\rangle = 4.1 \text{ J/cm}^2$ and $\langle\phi\rangle = 7.5 \text{ J/cm}^2$.

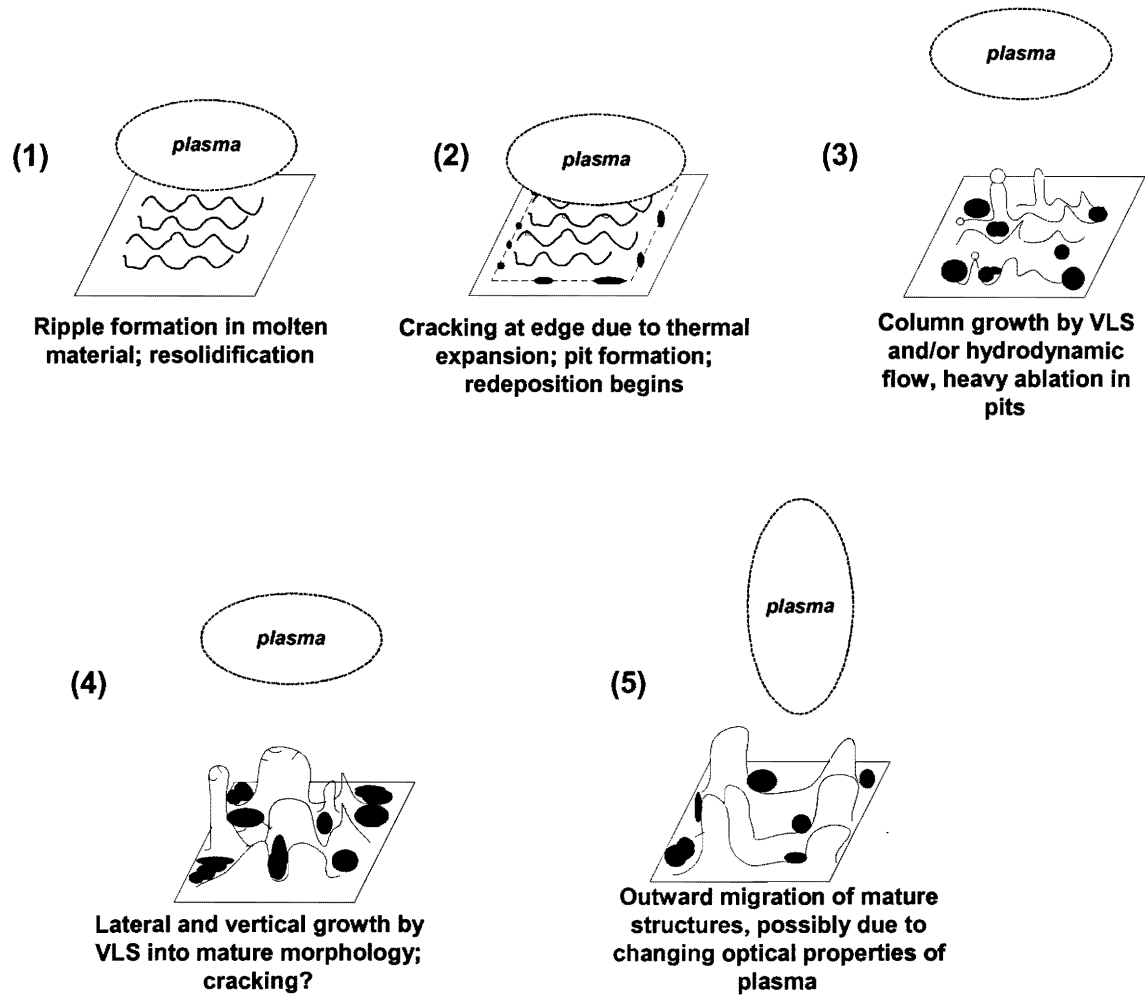


FIG. 17. Summary of microcolumn and tower formation mechanisms with increasing pulse number.

CONCLUSIONS

Microcolumn formation followed by tower growth was observed in specimens processed in vacuum in the fluence range $3.9 \text{ J/cm}^2 < \phi < 5.0 \text{ J/cm}^2$. At fluences lower than this, LIPSS form, apparently indefinitely, with amplitude proportional to the fluence and number of pulses. At fluences higher than approx. 5.0 J/cm^2 , a net loss of material occurs.

This formation appeared to result from the action of liquid globules in a manner consistent with the VLS mechanism. Pit formation and the roughening of LIPSS was also observed in each case where microcolumns formed. Microcolumns formed in vacuum have structures very similar to those formed in other processing atmospheres but become more irregular and larger. This may be due to the absence of etching in vacuum or a difference in the action of plasma in vacuum, but no observations have been made in this work to confirm or deny the latter conjecture.

Mature structures in vacuum have a "tower" morphology. This seems to be due to the presence of multiple liquid redeposition sites on microcolumns which become towers, the merger of neighboring microcolumns through the conjunction of the liquid droplets where growth is occurring, or both.

Growth terminates after a certain number of pulses. Cracks are observed in the tallest towers. This is probably the result of shockwaves originating from the plasma over the surface of the specimen.

Samples processed in vacuum also have low reflectivity and thus may be classified as "black silicon" as the difference to the unaided eye is not pronounced.

FUTURE WORK

This work should be reproduced more thoroughly with an improved optical arrangement that homogenizes the beam and with more accurate fluence determination.

Samples processed in vacuum so as to produce towers should be reprocessed in a reactive environment (*e.g.* air) to determine if towers may be reduced in size, if further growth may be stimulated, or if unexpected morphologies result. Likewise, specimens processed in air or SF₆ should be reprocessed in vacuum to determine if morphologies similar to those reported in this work result.

Materials other than Si such as Ge and other semiconducting materials should be irradiated in vacuum to determine the resulting topology.

REFERENCES

- ¹S. R. Foltyn, in *Pulsed Laser Deposition of Thin Films*, D. B. Chrisey and G. K. Hubler, eds. (New York: Wiley-Interscience, 1994), 90-103.
- ²H. M. van Driel, J. E. Sipe, and J. F. Young, *Phys. Rev. Lett.* **49**, 1955-1958 (1982).
- ³R. S. Taylor, K. E. Leopold, D. L. Singleton, G. Paraskevopoulos, and R. S. Irwin, *J. Appl. Phys.* **64**, 2815 (1988).
- ⁴J. E. Rothenberg and R. Kelly, *Nucl. Instrum. Meth.* **B1**, 291 (1984).
- ⁵“Spiky Silicon,” *Scientific American*, 22 March 1999 [journal online]; available from <http://www.scientificamerican.com/exhibit/1999/032299silicon/index.html>; Internet; accessed 3 April 1999.
- ⁶A. J. Pedraza, private communication (1998).
- ⁷E. I. Givargizov, A. N. Kiselev, L. N. Obolenskaya, and A. N. Stepanova, *Appl. Surf. Sci.* **67**, 74 (1992).
- ⁸F. Sánchez, J. L. Morenza, R. Aguiar, J. C. Delgado, and M. Varela, *Appl. Phys. A* **66**, 83 (1998).
- ⁹F. Sánchez, J. L. Morenza, R. Aguiar, J. C. Delgado, and M. Varela, *Appl. Phys. Lett.* **69**, 621 (1996).
- ¹⁰*Ibid.*, 622.
- ¹¹F. Sánchez, J. L. Morenza, R. Aguiar, J. C. Delgado, and M. Varela, *Appl. Phys. A* **66**, 85 (1998).
- ¹²J. Fowlkes, thesis, University of Tennessee, Knoxville (1999).
- ¹³F. Sánchez, J. L. Morenza, R. Aguiar, J. C. Delgado, and M. Varela, *Appl. Phys. A* **66**, 86 (1998).
- ¹⁴T-H. Her, R. J. Finlay, C. Wu, S. Deliwala, and E. Mazur, *Appl. Phys. Lett.* **73**, 1673 (1998).
- ¹⁵M. F. von Allmen and S. S. Lau, in *Laser Annealing of Semiconductors*, J. M. Poate and J. W. Mayer, eds. (New York: Academic Press, 1982), 564.
- ¹⁶T-H. Her, R. J. Finlay, C. Wu, S. Deliwala, and E. Mazur, *Appl. Phys. Lett.* **73**, 1674 (1998).
- ¹⁷“Spiky Silicon,” 1.
- ¹⁸E. I. Givargizov, in *Current Topics in Materials Science*, E. Kaldis, ed. (Amsterdam: North-Holland, 1978), v. 1, 86.
- ¹⁹A. J. Pedraza, J. D. Fowlkes, and D. H. Lowndes, *Appl. Phys. Lett.* **74**, 2324 (1999).
- ²⁰A. W. Bailey and A. Modak, *J. Thermophysics* **3**, 42 (1989).
- ²¹R. K. Singh and J. Narayan, in *Plasma and Laser Processing of Materials*, K. Upadhy, ed. (Warrendale, PA: TMS, 1991), 334.
- ²²G. B. Shinn, F. Steigerwalk, H. Stiegler, R. Sauerbrey, F. K. Tittel, and W. L. Wilson, Jr., *J. Vac. Sci. Technol. B.* **4**, 1276 (1986).
- ²³E. I. Givargizov, in *Current Topics in Materials Science*, E. Kaldis, ed. (Amsterdam: North-Holland, 1978), v. 1, 122.
- ²⁴T-H. Her, R. J. Finlay, C. Wu, S. Deliwala, and E. Mazur, *Appl. Phys. Lett.* **73**, 1674 (1998).
- ²⁵F. Sánchez, J. L. Morenza, R. Aguiar, J. C. Delgado, and M. Varela, *Appl. Phys. Lett.* **69**, 621 (1996).